Networked Control of a Power System on Smart Grid: A Non-Uniform Sampling Approach

Raheel Javed, Ghulam Mustafa, Abdul Qayyum Khan, Muhammad Abid

Department of Electrical Engineering, Pakistan Institute of Engineering and Applied Sciences, Islamabad

Abstract

This article deals with the damping of low frequency power systems oscillations using a networked controller on smart grid. The network channel is assumed to be band-limited and has random delay whose probability distribution can be found. To mitigate the effect of delay on control system performance, the measurements from the system are sampled at a random and non-uniform period but the inputs are updated at a faster and constant rate. This makes the closed-loop control system a stochastic switching system. A framework to analyze mean square stability of the closed-loop system is developed and a switching observer-based controller is designed to ensure stability of the system at random sampling instants. A case study has been performed using the Western-System-Coordinating-Council (WSCC) 3-machines, 9-bus system for verification of the technique. The contribution of the paper is a bandwidth efficient delay compensation technique and its application to power systems stability enhancement in smart grid.

Keywords: Smart Grid, Thyristor Controlled Series Capacitor, Rotor Angle Stability, Networked Control System, Non-Uniform Sampling, Stochastic Switching System, Mean Square Stability, Switching Stability, Cone Complementarity Linearization Algorithm, Linear Matrix Inequalities

1. Introduction

One of the phenomena inherent in forming a power system network is the existance of low frequency electro-mechanical oscillations that may arise when the system is disturbed from its equilibrium position. They may be classified as intra-plant mode, local-plant mode and inter-area mode, etc., based on their origin and part of the network being affected [1]. They may be triggered by the disturbances due to load changes in the system or a momentarily fault on a tie-line and may cause instability if persists-for a longer duration. These oscillations must be damped to prevent power outage due to large power variations. A mean to control these oscillations is to use a Flexible AC Transmission System (FACTS) controller, such as, Thyristor Controlled Series Capacitor (TCSC). TCSC acts as a variable reactance which is controlled by firing angle of a thyrister. It is usually installed at a tie-line in the power system network and can control multiple modes simultaneously.

Various methods have been employed to control the oscillations [2, 3]. In [2], authors use controlled series compensation to improve stability of multi-machine power system. They provide a technique to choose a suitable location for series compensation based on residue analysis and design a damping controller using the pole placement technique. In [3], Linear Quadratic Regulator (LQR) and robust Linear Quadratic Gaussian (LQG) controls for TCSC are presented to control power system oscillations. The designed controllers are verified on Western System Coordinating Council (WSCC) 3-machines, 9-bus system.

The conventional electrical grid has been modernized into smart grid which has enabled the integration of communication and IT infrastructure [4]. It has made possible to employ networked controlled systems to enhance power systems stability [5]. Networked controlled systems have the advantages of easier installation, flexibility, lower cost, easier maintenance and reliability. But the use of a networked controller poses challenges, such as, bandwidth limitations, delays in the channel, packets dropout, packets disordering and corruption, etc., which may degrade the performance of closed-loop control or cause instability. These issues have been addressed in literature [6, 7]. In [6], stability analysis is performed for a networked control system on smart grid where the channel has random packets dropout, modeled by the Bernoulli's random process. An LQG control is synthesized for TCSC to damp power system oscillations. In [8], a speed controller is designed for networked DC motor in the presence of channel delays and packet losses. Zero steady state error and stability conditions are derived and estimation for distribution algorithm is used for optimization of controller parameters. In [7], an LMI-based controller is developed based on wide area measurements. The communication effects like time delays, packets dropout and disordering have been considered by incorporating time varying delays in system model. In [9], authors have given the concept of observer-driven system copy to design control on a constrained bandwidth network. It uses the nominal system model to generate measurement data when data from Phasor Measurement Units (PMUs) is not available.

Different applications are being implemented in Smart Grid like state estimation, transient stability, small signal stability and voltage stability [10]. Each application has different com-

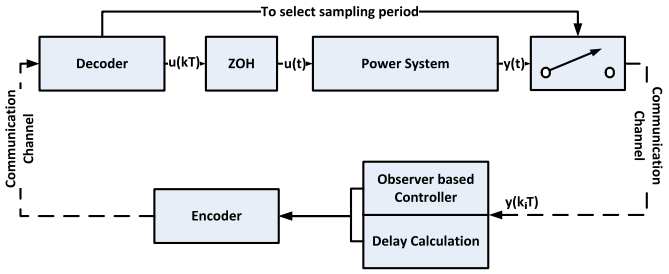

Figure 1: A non-uniformly sampled networked control system on Smart Grid

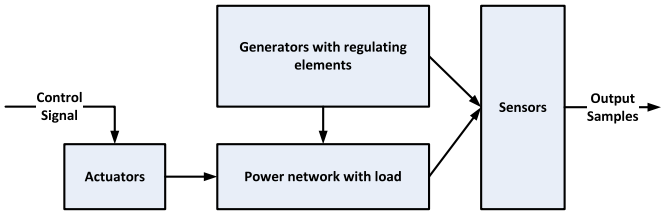

Figure 2: Inside a power system block

munication requirements [11, 12]. If a shared channel is used for communication, it may cause delays due to network congestion. The same problem may arise if a channel with limited bandwidth is used or some links in the channel are offline. In this case, a control strategy is required that ensures stability of the control system and at the same time efficiently uses channel bandwidth.

This article addresses the aforementioned two network constraints. A conference paper [13] by the same authors discusses the rotor angle stability enhancement over a random delayed network. It designs a Kalman filter based optimal stochastic control with no bandwidth constraint. The method holds only if the sum of delays is not greater than the sampling period of the system but the article presented here has no such limitation. This paper presents an idea to deal with random delay that may arise on a band-limited channel and the delay can be greater than the system sampling time. A switching observer-based controller is designed to damp the oscillations. The idea is to sample the system measurements at a random and variable period to minimize the effect of delay on the system. However, the use of non-uniform sampling period makes the system a stochastic switching system because it switches to different sampling periods. Stability analysis of closed-loop system is performed to investigate the effects of change in delay probabilities and model parameters on system stability. Simulation results show that the proposed control provides sufficient damping to the oscillations even with variations in power system model and delay profile.

The paper is organized follows: In section 2, a generalized model of power system is described and its simplification to the form used for design purposes is presented. Assumptions about the network channel are made and the plant is discretized at a random sampling period. Structure of observer and controller is chosen in section 3 and stability analysis of the stochastic switching system is performed. Section 4 deals with the design of an observer based controller that takes non-uniformly sampled measurements to give control signal at a fast and constant rate. Also, the procedure for switching the observer based controller is defined. Section 5 provides the method to choose sampling periods based on delay profile. Section 6 presents a case study using WSCC 3-machines, 9-bus power system to verify the performance of the proposed controller and observer. Section 7 concludes the paper.

2. Problem Formulation

Consider a scenario of networked control on Smart Grid as shown in Figure 1. Where, the power system block represents the oscillatory dynamics to be controlled. The measurements, $y(t)$, from the power system are sampled and sent to the controller through a shared communication network. The communication channel is assumed to be band-limited with random communication delay. In order to compensate for delay and to efficiently utilize the channel bandwidth, a non-uniform sampling strategy is adopted. The sampler which is adaptive in nature has an extra input for time in seconds which is hard-wired to the decoder block. The sampler switches the sampling period according to the input signal. It is assumed that the delay can be measured online by time stamping the packets or by sending dummy packets between the measurement samples. The delay measurements are used to decide the period after which next sample will be taken. A mapping technique from range of delay to sampling period is given in section 5. The delay calculation and mapping is performed in the period calculation block. The controller is an observer-based one with dynamics switching with the sampling period. The block is event driven meaning it will update it's operation whenever a measurement packet is received. The controller output together with the sampling period is encoded into a single packet via the encoder block and sent to the plant. A decoder block on the plant side separates the sampling period and control input. The control input is applied to the plant via a zero-order-hold which holds the current sample value until next packet has arrived and the sampler adapts the sampling period.

2.1. Power System Modeling

The power system block on the inside consists of generators, actuators, sensors and power network as shown in Fig. 2. The generator includes the dynamics of AC machine along with exciter, power system stabilizer, automatic voltage regulator and speed governor. The generators are connected to power transmission network which also models transformers and loads connected to the transmission lines. The actuators (FACTS controller, like, TCSC) take input from the control element and act as a variable reactance on a tie line in the power network.

Fig. 3 shows circuit of TCSC, the inputs and outputs are connected within the power network such that it is in series on a tie line, whereas, the firing angles of thyristers are provided by the controller. The dynamics are modeled by a first order

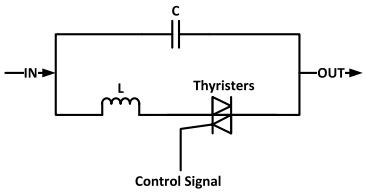

Figure 3: Circuit diagram of TCSC

differential equation [2] along with the parameters that are later used in case study.

$$\dot{X_c} = \frac{1}{T_c}(-X_c + X_u), \;\; X_{cmin} < X_c < X_{cmax} \tag{1}$$

where X_c is reactance of TCSC, T_c is the time constant in seconds and X_u is the input signal to TCSC which serves as a reference for output reactance. X_{cmax} and X_{cmin} are the maximum and minimum limits of reactance of TCSC.

The sensors in the power system usually include Current Transformers (CTs) and Potential Transformers (PTs). In the context of Smart Grid, Phasor Measurement Units (PMUs) to sample and transmit the condition of power network in real time are also included. Due to availability of a communication network the position and speed of the connected machines may also be monitored for the purpose of power system stability. A generalized model of power system including actuator can be represented as a set of differential algebraic equations

$$\begin{aligned} \dot{x_f}(t) &= f(x_f(t), y(t), u(t)) \\ 0 &= g(x_f(t), y(t)) \end{aligned} \tag{2}$$

where $x_f(t) \in R^{n_f}$ represents state vector, $y(t) \in R^m$ represents output vector, $u(t) \in R^{k_u}$ represents input vector, t represents time in seconds, $f : R^{n_f} \times R^m \times R^{k_u} \rightarrow R^{n_f}$ is a non-linear function of states, inputs, outputs and $g : R^{n_f} \times R^m \times \rightarrow R^{bm}$ is a non-linear function of states and time. For a power network $bm = 2\times$(no. of buses + no. of machines).

The location of TCSC in the power system can be chosen by following residue analysis. It is based on choosing that position for TCSC which gives largest residue for the oscillatory modes, when the system transfer function is represented as partial fraction expansion. The procedure is mentioned in [2]. The output of plant can be selected using the concept of mode observability [14]. This will ensure that modes to be controlled are observable from the chosen system output. For design purpose, the plant model is usually linearized about an operating point and its number of states is reduced keeping the modes to be controlled dominant in reduced system [3]. A method for model reduction can be seen in [15]. The reduced model takes the form

$$\begin{aligned} \dot{x}(t) &= A_c x(t) + B_c u(t) \\ y(t) &= C x(t) \end{aligned} \tag{3}$$

where $x(t) \in R^n$ is the reduced state vector, $y(t) \in R^m$ is the output vector and $A_c \in R^{n\times n}$, $B_c \in R^{n\times k_u}$, and $C \in R^{m\times n}$ are matrices of compatible dimensions. To see effects of different

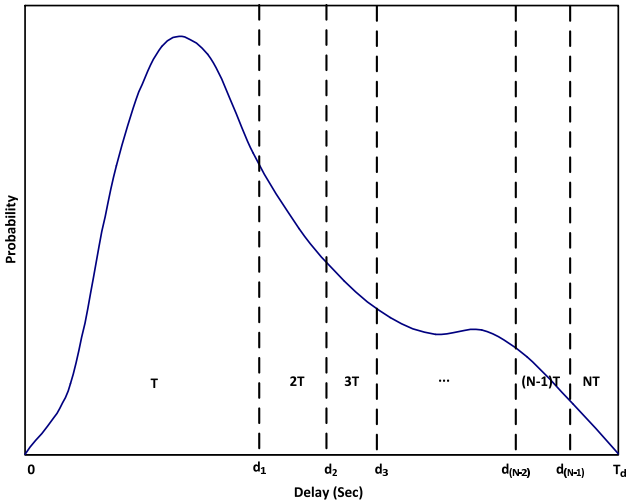

Figure 4: General delay profile of network

dynamics (eigenvalues) on the states of power system, participation factors are calculated as in [16]:

$$p_{ki} = \frac{|v_{ik}||w_{ik}|}{\sum_{k=1}^{n} |v_{ik}||w_{ik}|} \tag{4}$$

Here w_i and v_i are the left eigenvector and right eigenvector corresponding to ith eigenvalue of A_c; respectively, and w_{ik} and v_{ik} are kth elements of ith eigenvectors.

2.2. Communication Network

The feedback loop of the system contains two communication networks. It is supposed that the network between plant and controller is shared and band-limited, having random transmission delay. The delay may be due to queuing in the network or re-transmission if a packet is lost. To keep the channel model simple and general, it is further assumed that the delay is independent of its previous value. The network between controller and actuator is assumed to have negligible delay. The probability distribution of the delay can be obtained by pre-testing the channel as shown in Fig. 4. This can be done by recording end-to-end delay measurements of the channel before commissioning and plotting the results based on frequency of occurrence.

The maximum value of delay is limited to T_d. The delay is divided into N partitions and to each a suitable sampling period is assigned which will reduce the effect of delay in that range. If delay is much smaller than the sampling period of the system then it can be neglected due to lesser effect on the performance of system. Section 5 describes a way to choose partitions and assigning sampling periods to them based on minimizing the error between delayed and non-delayed plant model. Then the sampling time adaptation can be achieved as follows:

- The packet $y(k_iT)$ is time stamped at the plant side of the closed-loop system.
- At the controller side, an additional block of period calculation is added which uses the time data from the packet to calculate the current channel delay and maps it to a sampling period.

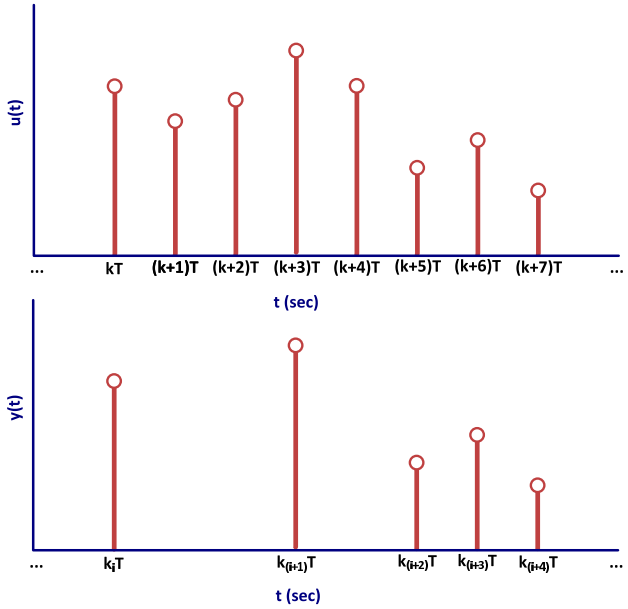

Figure 5: Non-uniform sampling

- The calculated sampling period is then encoded with the control packet and sent to the plant side.
- At the plant side, the decoder is used to separate the sampling period from the packet.
- The sampler will then adapt the sampling period and decide when the next measurement samples will be transmitted.

Note that in Fig. 4, a faster sampling period T is assigned to the first partition. It is the basic sampling period of system when there is negligible channel delay. The rest of the periods are integer multiples of T. This makes the development of case convenient and leads to a simple design of sampler.

2.3. Non-Uniformly Sampled System

Since, the sampling time of the system is being changed by delay measurments in real time, there may be cases in which the period exceeds the minimum required to stabilize the system. To compensate for that, the input to the power system is updated at a faster sampling period T, $[kT, (k+1)T, \ldots]$ [17] whereas the measurement is sampled with non-uniform periods $[k_iT, k_{i+1}T, \ldots]$ as shown in Fig. 5. The non-uniform and random sampling of the output makes the system a stochastic switching system with N independent switching modes. Each mode will be represented by a different sampling period and the probability of occurrence of a mode will be defined by the probability of delay lying in a specific range.

To consider the effect of non-uniform sampling instants, the model is discretized at random sampling periods jT, where, $j = k_{i+1} - k_i = 1, 2, \ldots, N$ is a random variable which represents the current sampling period. Since the delay varies randomly and so do the sampling periods. The probability distribution of j can be found from the delay profile and can be written as $P(j = 1) = p_1$, $P(j = 2) = p_2$, $\ldots$, $P(j = N) = p_N$, where, $p_1, p_2, \ldots, p_N$ are the probabilities of delay lying in partitions $1, 2, \ldots, N$; respectively. The discretization process is performed by solving the continuous time differential equation (3) and is summarized as [18]:

$$\begin{aligned} x(k_{i+1}T) &= e^{jA_cT}x(k_iT) + \int_{k_iT}^{k_{i+1}T} e^{A_c(k_{i+1}T-\tau)}B_cu(\tau)\,d\tau \\ &= e^{jA_cT}x(k_iT) + \int_{k_iT}^{(k_i+1)T} e^{A_c(k_{i+1}T-\tau)}B_cu(k_iT) \\ &\quad d\tau + \int_{(k_i+1)T}^{(k_i+2)T} e^{A_c(k_{i+1}T-\tau)}B_cu((k_i+1)T)\,d\tau + \\ &\quad \ldots + \int_{(k_{i+1}-1)T}^{k_{i+1}T} e^{A_c(k_{i+1}T-\tau)}B_cu((k_{i+1}-1)T)\,d\tau \end{aligned}$$

Using change of variables $t_1 = (k_i+1)T-\tau$, $t_2 = (k_i+2)T-\tau$, $\ldots$, $t_j = (k_{i+1})T - \tau$, the following form is obtained:

$$\begin{aligned} x(k_{i+1}T) &= e^{jA_cT}x(k_iT) + \int_0^T e^{A_c(jT-T+t_1)}B_cu(k_iT)\,dt_1 \\ &\quad + \int_0^T e^{A_c(jT-2T-t_2)}B_cu((k_i+1)T)\,dt_2\ \ldots \\ &\quad + \int_0^T e^{A_ct_j}B_cu((k_{i+1}-1)T)\,dt_j \end{aligned}$$

The above equation can be written in compact form by representing all terms containing input samples in vector form and changing constant terms by an easier notation as follows:

$$x_{k_{i+1}} = A^j x_{k_i} + \begin{bmatrix} B & AB & \ldots & A^{j-1}B \end{bmatrix} \begin{bmatrix} u_{k_{i+1}-1} \\ u_{k_{i+1}-2} \\ \vdots \\ u_{k_i} \end{bmatrix} \tag{5}$$

where, $A \in R^{n\times n}$ and $B \in R^{n\times k_u}$ are matrices from the plant sampled at faster period T, given as

$$\begin{aligned} A &= e^{A_cT} \\ B &= \int_0^T e^{A_ct}B_c\,dt \end{aligned}$$

Problem: Design a stabilizing controller for the power system represented in (5) such that the oscillatory modes are stabilized and well-damped.

Note that the pair (A, B) should be stabilizable and the pair (A, C) should be detectable, that is, the system with period T should be stabilizable and detectable for the non-uniformly sampled system to be observable and controllable. It follows from the fact that it is the mode at which the stochastic switching system will be operating more than any other mode and it is chosen to capture the oscillatory dynamics of the power system as shown in section 5.

3. Analysis of Stochastic Switching System

A framework to analyze stability of closed-loop system with observer is developed to investigate the effects of different factors like change in delay, delay probabilities, parameters of observer, controller and power system. For stability analysis of the closed-loop system, the structure of controller and observer is required. The proposed controller and observer structures are given as follows:

3.1. Controller

To control the random and non-uniformly sampled system, a switching controller is used. This will make the problem of finding a stabilizing controller lesser constrained than a fixed controller design. The controller gain matrix will change its value based on the time after which an output measurement is received. Thus, the control applied to the system will also be switching in random manner based on the sampling period of the system. Since, input to the plant is updated at a faster sampling period T, the controller also operates at that period. To design a state feedback controller, the following structure for controller is used:

$$u_k = F\hat{x}_k$$

where, $F \in R^{k_u \times n}$ is the state feedback gain matrix. Keeping in view that the current system state is function of j number of input samples as shown in (5), the controller takes the form

$$\begin{aligned} u_{k_i} &= F_1\hat{x}_{k_i} \\ u_{k_i+1} &= F_2\hat{x}_{k_i+1} \\ &\vdots \\ u_{k_{i+1}-1} &= F_j\hat{x}_{k_{i+1}-1} \end{aligned} \tag{6}$$

3.2. Observer

Since states of the power system are unavailable between instants $k_{i+1}T$ and k_iT, an observer is used to estimate the state vector. The measurement samples are received in a non-uniform manner and the input to plant is updated at a faster sampling period T, the observer also provides the states at period T. In this case a good strategy is to correct the error between observer and system states only at the instant when output measurement is sampled and received at observer. Any disturbance acting upon the system between the sampled measurements will be detected on the next measurement sample. A switching structure is also used for the observer in which observer gain matrix takes a value based on the number of faster samples after which an output measurement will be received. A structure for such an observer can be written as [19]

$$\hat{x}_{k+1} = A\hat{x}_k + Bu_k + \phi L(y_k - \hat{y}_k) \tag{7}$$

where ϕ is equal to 1 if an output sample is received and 0; otherwise, $L \in R^{n \times m}$ is the observer gain matrix. In the current scenario, the observer will be change its gain based on the switching mode of the plant. So, using the assumption of negligible delay effect, the equation in (7) can be modified as

$$\begin{aligned} \hat{x}_{k_i+1} &= A\hat{x}_{k_i} + Bu_{k_i} + L_j(Cx_{k_i} - C\hat{x}_{k_i}) \\ \hat{x}_{k_i+2} &= A\hat{x}_{k_i+1} + Bu_{k_i+1} \\ &\vdots \\ \hat{x}_{k_{i+1}} &= A\hat{x}_{k_{i+1}-1} + Bu_{k_{i+1}-1} \end{aligned} \tag{8}$$

which can be combined in the following form

$$\begin{aligned} \hat{x}_{k_{i+1}} &= A^{j-1}\hat{x}_{k_i} + A^{j-1}L_jC(x_{k_i} - \hat{x}_{k_i}) \\ &\quad + \begin{bmatrix} B & AB & \dots & A^{j-1}B \end{bmatrix} \begin{bmatrix} u_{k_{i+1}-1} \\ u_{k_{i+1}-2} \\ \vdots \\ u_{k_i} \end{bmatrix} \end{aligned} \tag{9}$$

3.3. Stability Analysis

For stability analysis, the closed-loop system is formed by augmenting observer states to the plant states and then closing the loop with controller. The stability of the system will then guarantee that the states of observer and plant will be bounded. Using (5), (6) and (8), the following form of the augmented system is obtained:

$$\tilde{x}_{k_{i+1}} = \mathcal{A}_j\tilde{x}_{k_i} \tag{10}$$

where $\tilde{x}_{k_i} = \begin{bmatrix} x_{k_i} & \hat{x}_{k_{i+1}-1} & \dots & \hat{x}_{k_i+1} & \hat{x}_{k_i} \end{bmatrix}$ and

$$\mathcal{A}_j = \begin{bmatrix} A^j & BF_j & \dots & A^{j-2}BF_2 & A^{j-1}BF_1 \\ 0 & A + BF_{j-1} & \dots & 0 & 0 \\ \vdots & \vdots & \ddots & \vdots & \vdots \\ 0 & 0 & \dots & A + BF_2 & 0 \\ L_jC & 0 & \dots & 0 & A + BF_1 - L_jC \end{bmatrix}.$$

$\mathcal{A}_j$ can be written in following form to facilitate analysis

$$\mathcal{A}_j = \mathbf{A}_j + \mathbf{B}_j\mathbf{F}_j + \mathbf{L}_j\mathbf{C}_j \tag{11}$$

where

$$\mathbf{A}_j = \begin{bmatrix} A^j & 0 & \dots & 0 & 0 \\ 0 & A & \dots & 0 & 0 \\ \vdots & \vdots & \ddots & \vdots & \vdots \\ 0 & 0 & \dots & A & 0 \\ 0 & 0 & \dots & 0 & A \end{bmatrix}$$

$$\mathbf{B}_j = \begin{bmatrix} 0 & B & \dots & A^{j-2}B & A^{j-1}B \\ 0 & B & \dots & 0 & 0 \\ \vdots & \vdots & \ddots & \vdots & \vdots \\ 0 & 0 & \dots & B & 0 \\ 0 & 0 & \dots & 0 & B \end{bmatrix}$$

$$\mathbf{F}_j = \begin{bmatrix} 0 & 0 & \dots & 0 & 0 \\ 0 & F_j & \dots & 0 & 0 \\ \vdots & \vdots & \ddots & \vdots & \vdots \\ 0 & 0 & \dots & F_2 & 0 \\ 0 & 0 & \dots & 0 & F_1 \end{bmatrix}$$

$$\mathbf{C}_j = \begin{bmatrix} 0 & 0 & \dots & 0 & 0 \\ 0 & 0 & \dots & 0 & 0 \\ \vdots & \vdots & \ddots & \vdots & \vdots \\ 0 & 0 & \dots & 0 & 0 \\ C & 0 & \dots & 0 & -C \end{bmatrix}$$

$$\mathbf{L}_j = \begin{bmatrix} 0 & 0 & \dots & 0 & 0 \\ 0 & 0 & \dots & 0 & 0 \\ 0 & 0 & \dots & 0 & 0 \\ \vdots & \vdots & \ddots & \vdots & \vdots \\ 0 & 0 & \dots & 0 & 0 \\ 0 & 0 & \dots & 0 & L_j \end{bmatrix}$$

and the augmented closed-loop system can be finally represented as

$$\tilde{x}_{k_{i+1}} = \left(\mathbf{A}_j + \mathbf{B}_j\mathbf{F}_j + \mathbf{L}_j\mathbf{C}_j\right)\tilde{x}_{k_i} \tag{12}$$

Lyapunov theory is used to analyze the closed-loop system. The conditions are formulated as LMI constraints guaranteeing stochastic stability of the closed-loop system. This definition of stability takes into account the probability of the system jumping randomly from one mode to another. The following theorem can be used to perform analysis of the switching system:

Theorem 1. *The closed loop system in* (12) *will be mean square stable, i.e.,* $\lim_{i\to\infty} E[\tilde{x}_{k_i}] = 0$*, if there exist symmetric* $R_l > 0$ *for* $l = 1, 2, \dots, N$ *such that the following LMI constraints are satisfied:*

$$\begin{bmatrix} R_l & (\mathcal{A}_1 R_l)^T & (\mathcal{A}_2 R_l)^T & \dots & (\mathcal{A}_N R_l)^T \\ * & p_1^{-1}R_1 & 0 & \dots & 0 \\ * & * & p_2^{-1}R_2 & \dots & 0 \\ * & * & * & \ddots & 0 \\ * & * & * & * & p_N^{-1}R_N \end{bmatrix} > 0 \tag{13}$$

Proof. Consider the following Lyapunov function

$$W_{k_i} = \tilde{x}_{k_i}^T R_l \tilde{x}_{k_i} > 0, \;\; l = 1, 2, \dots, N$$

where, R_l is symmetric and postive definite. To ensure that the closed-loop system will be mean square stable, i.e., $\lim_{i\to\infty} E[\tilde{x}_{k_i}] = 0$, it is required that [20]:

$$E[\Delta W] < 0 \tag{14}$$

$$E[W_{k_{i+1}}] - W_{k_i} < 0 \tag{15}$$

$$\begin{aligned} \tilde{x}_{k_i}^T [p_1 \mathcal{A}_1^T Q_1 \mathcal{A}_1 + p_2 \mathcal{A}_2^T Q_2 \mathcal{A}_2 + \\ \dots + p_N \mathcal{A}_N^T Q_N \mathcal{A}_N - Q_l] \tilde{x}_{k_i} < 0 \end{aligned} \tag{16}$$

Applying Schur's complement to the above case leads to the following matrix inequalities:

$$\begin{bmatrix} Q_l & \mathcal{A}_1^T & \mathcal{A}_2^T & \dots & \mathcal{A}_N^T \\ * & p_1^{-1}Q_1^{-1} & 0 & \dots & 0 \\ * & * & p_2^{-1}Q_2^{-1} & \dots & 0 \\ * & * & * & \ddots & 0 \\ * & * & * & * & p_N^{-1}Q_N^{-1} \end{bmatrix} > 0 \tag{17}$$

Performing congruence transformation with

$$diag(Q_l^{-1}, 0, 0, \dots, 0) \tag{18}$$

and substituting $R_l = Q_l^{-1}$, (13) is obtained.

4. Design of Observer-based Controller

From (13), it can be seen that if $\mathbf{L}_j$ and $\mathbf{F}_j$ are both treated as variables, the LMI becomes a non-convex problem and hence harder to solve. But, the separation principle holds here, which means the controller and observer can be designed independently. The proof of separation principle is given in appendix. $\mathbf{L}_j$ and $\mathbf{F}_j$ then calculated will guarantee that the closed loop system with observer becomes mean square stable. To design the controller, the closed-loop system representation is obtained by inserting (6) in (5),

$$x_{k_{i+1}} = A^j F_1 x_{k_i} + \begin{bmatrix} B & AB & \dots & A^{j-1}B \end{bmatrix} \begin{bmatrix} F_j x_{k_{i+1}-1} \\ F_{j-1} x_{k_{i+1}-2} \\ \vdots \\ F_1 x_{k_i} \end{bmatrix}$$

which can be finally written in a compact form as

$$\bar{x}_{k_{i+1}} = \bar{A}_j \bar{x}_{k_i} \tag{19}$$

where

$$\bar{x}_{k_{i+1}} = \begin{bmatrix} x_{k_{i+1}} \\ x_{k_{i+1}-1} \\ \vdots \\ x_{k_i+2} \\ x_{k_i+1} \end{bmatrix}, \;\; \bar{x}_{k_i} = \begin{bmatrix} x_{k_{i+1}-1} \\ x_{k_{i+1}-2} \\ \vdots \\ x_{k_i+1} \\ x_{k_i} \end{bmatrix}$$

$$\bar{A}_j = \begin{bmatrix} BF_j & ABF_{j-1} & \dots & A^{j-2}BF_2 & A^j + A^{j-1}BF_1 \\ I_n & 0 & \dots & 0 & 0 \\ \vdots & \ddots & \vdots & \vdots & \vdots \\ 0 & 0 & \ddots & 0 & 0 \\ 0 & 0 & \dots & I_n & 0 \end{bmatrix}$$

Where, I_n is an identity matrix of size $n \times n$. $\bar{A}_j$ can be decomposed into a form appropriate for finding state feedback gain matrices:

$$\bar{A}_j = \tilde{A}_j + \tilde{B}_j \tilde{F}_j \tag{20}$$

Where

$$\tilde{A}_j = \begin{bmatrix} 0 & 0 & \dots & 0 & A^j \\ I_n & 0 & \dots & 0 & 0 \\ \vdots & \ddots & \vdots & \vdots & \vdots \\ 0 & 0 & \ddots & 0 & 0 \\ 0 & 0 & \dots & I_n & 0 \end{bmatrix},$$

$$\tilde{B}_j = \begin{bmatrix} B & AB & \dots & A^{j-2}B & A^{j-1}B \\ 0 & 0 & \dots & 0 & 0 \\ \vdots & \vdots & \vdots & \vdots & \vdots \\ 0 & 0 & \dots & 0 & 0 \\ 0 & 0 & \dots & 0 & 0 \end{bmatrix}$$

$$\tilde{F}_j = \begin{bmatrix} F_j & 0 & \dots & 0 & 0 \\ 0 & F_{j-1} & \dots & 0 & 0 \\ \vdots & \vdots & \ddots & \vdots & \vdots \\ 0 & 0 & \dots & F_2 & 0 \\ 0 & 0 & \dots & 0 & F_1 \end{bmatrix}$$

Note that the dimensions of above matrices will change for different values of j (different modes), so, I_n and 0 should be inserted at appropriate places in the matrices to make the dimensions compatible for different values of j. Finally, the closed-loop system can be represented as:

$$\bar{x}_{k_{i+1}} = \left(\tilde{A}_j + \tilde{B}_j \tilde{F}_j\right) \bar{x}_{k_i} \tag{21}$$

To design a controller stabilizing the closed loop system, an LMI based solution is obtained guaranteeing stochastic switching stability of the system. Following theorem can be used to find the controller gain matrices:

Theorem 2. *The closed-loop system in* (21) *is mean square stable i.e.* $\lim_{i\to\infty} E[x_{k_i}] = 0$*, if symmetric* $T_1 > 0, T_2 > 0, \dots, T_N > 0$ *and* $X_1, X_2, \dots, X_N$ *can be found such that the following LMI constraints are satisfied:*

$$\begin{bmatrix} T_l & \mathcal{E}_1^T & \mathcal{E}_2^T & \dots & \mathcal{E}_N^T \\ * & T_1 & 0 & \dots & 0 \\ * & * & T_2 & \dots & 0 \\ * & * & * & \ddots & 0 \\ * & * & * & * & T_N \end{bmatrix} > 0,\ l = 1, 2, \dots, N$$

Where,

$$\begin{aligned} \mathcal{E}_1 &= \sqrt{p_1}\left(\tilde{A}_1 T_l + \tilde{B}_1 X_l\right) \\ \mathcal{E}_2 &= \sqrt{p_2}\left(\tilde{A}_2 T_l + \tilde{B}_2 X_l\right) \\ \mathcal{E}_N &= \sqrt{p_N}\left(\tilde{A}_N T_l + \tilde{B}_N X_l\right) \end{aligned}$$

and $\tilde{F}_j T_l = X_l$.

The proof of the theorem is straight forward and can be done by following same steps as theorem 1. Now, to design observer, the error system must be stabilized. The dynamics of the error system can be described by inserting (6) in (9) and subtracting from (5) to give

$$e_{k_{i+1}} = \hat{A}_j e_{k_i}, \tag{22}$$

where $e_{k_i} = x_{k_i} - \hat{x}_{k_i}$, $\hat{A}_j = A^j - A^{j-1} L_j C$ and L_j are the observer gain matrices. The error system does not depend on the controller gain matrices which means that the observer can be designed independently. Switching stability is guaranteed by L_j for any mode of the error system whatever the probability of that mode is. This will give a constrained solution for observer but a better one from point of view of response as the response between the measurement samples greatly depends upon the accuracy of observer. The following theorem can be used to find observer gain matrices:

Theorem 3. *The error system in* (22) *is switching stable for all N modes irrespective of their probabilities of occurrence, if symmetric* $P_1 > 0, P_2 > 0, \dots, P_N > 0, S_1 > 0, S_2 > 0, \dots, S_N > 0$ *and* $L_1, L_2, \dots, L_N$ *can be found which satisfy the following LMI constraints:*

$$\begin{bmatrix} P_l & \hat{A}_q^T \\ * & S_q \end{bmatrix} > 0 \tag{23}$$

$$\begin{bmatrix} P_l & 0 \\ * & S_l \end{bmatrix} > 0 \tag{24}$$

subjected to the objective function

$$\min\ trace(P_1 S_1 + P_2 S_2 + \dots + P_N S_N) \tag{25}$$

where $l = 1, 2, \dots, N$ *and* $q = 1, 2, \dots, N$.

Proof. Consider a Lyapunov function,

$$V_{k_i} = e_{k_i}^T P_l e_{k_i} > 0,\ \ l = 1, 2, \dots, N \tag{26}$$

where P_l is symmetric and positive definite. To ensure switching stability from any mode l to q, we must have [21],

$$\begin{aligned} \Delta V &< 0 \\ V_{k_{i+1}} - V_{k_i} &< 0 \\ e_{k_i}^T [p_q \hat{A_q}^T P_q \hat{A_q} - P_l] e_{k_i} &< 0 \end{aligned}$$

Using Schur's complement, it leads to the following matrix inequalities

$$\begin{bmatrix} P_l & \hat{A}_q^T \\ * & P_q^{-1} \end{bmatrix} > 0 \tag{27}$$

The error system can be stabilized if $P_1, P_2, \cdots, P_N$ and $L_1, L_2, \cdots, L_N$ can be found such that the above matrix inequalities are satisfied. The matrix inequalities are non-convex and, hence, harder to solve. But a sub-optimal solution can be obtained by using Cone Complementarity Linearisation Algorithm (CCLA) [22]. Application of CCLA to the matrix inequalities (27) proves the theorem. It can be seen that the objective function given in theorem ensures that $P_1, P_2, \dots, P_N$ are inverses of $S_1, S_2, \dots, S_N$, respectively. The function is not linear, and thus not easier to solve, but it can be linearized and gain matrices can be obtained iteratively as shown in [22].

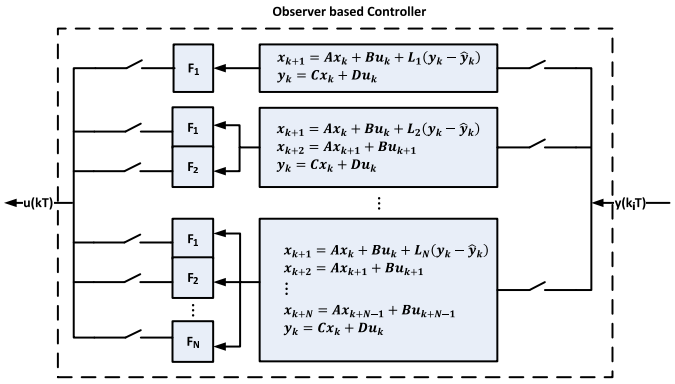

Figure 6: Internal structure of switching observer based controller

The structure of switching controller with observer is shown in Fig. 6. After implementation, following steps can be used for selecting online a combination of observer and controller based on the fact if a packet is received or not:

- The observer and ZOH block are event driven, so, they will update their output only when a packet is received.
- When a packet is received, the period calculation block calculates the value of j i.e., the duration (jT) after which the measurement will be received.
- The value of j decides the L_j. The corresponding block is engaged and correction is performed for the current measurement sample.
- The observer produces rest of the states without correction until a measurement is received keeping in view value of j.
- For switching of the controller, whenever a measurement packet is received, F_1 controller block is engaged.
- When a packet is not received after time T, the F_2 controller block is used. Similarly, F_3, F_4, ... , F_N will be used if the packet is not received after time $2T$, $3T$, ..., $(N-1)T$, respectively.

5. Selection of Sampling Period and Partitions of Delay Profile

The basic sampling period of system T can be calculated using Nyquist Criterion which states that the sampling frequency must be greater than twice the system bandwidth. Here, the system bandwidth is defined by the most oscillatory dynamic (eigenvalue having the largest imaginary part). Usually for the sake of performance the sampling frequency is set multiple of nyquist frequency, but, due to bandwidth constraint sampling frequency is set close to nyquist frequency. In case of poor performance the sampling frequency can be increased. The sampling period T then can be calculated as

$$T > \frac{\pi}{\text{imag}(\lambda_i)} \tag{28}$$

where imag() represents the imaginary part, λ_i is the eigenvalue with the largest imaginary part.

For design of observer based controller, an assumption has been made according to which selection of sampling period minimizes the effect of delay so that it can be neglected. This condition and the fact that system performance improves with smaller sampling periods with smaller delays is used to partition delay profile. An alternate representation of power system (5) with inputs also sampled non-uniformly as output can be written as,

$$x_{k_{i+1}} = A_j x_{k_i} + B_j u_{k_i} \tag{29}$$

where, A_j and B_j are system matrices obtained by discretizing continuous time system (3) at instant jT and x^o are undelayed power system states. The error between this system and a delayed version of it will be used for partitioning of delay profile. The delayed version with states $x^d_{k_i}$ when delay d is between 0 and jT can be written as,

$$\begin{aligned} x^d_{k_{i+1}} &= A_j x^d_{k_i} + \int_{k_iT}^{k_iT+d} e^{A_c(k_{i+1}T-\tau)} B_c\, u[(k_{i-1})T]d\tau + \\ &\quad \int_{k_iT+d}^{(k_{i+1})T} e^{A_c(k_{i+1}T-\tau)} B_c\, u(k_iT)d\tau \end{aligned}$$

which after variable substitution gives, [18]

$$\begin{aligned} x^d_{k_{i+1}} &= A_j x_{k_i} + e^{A_c(jT-d)} \int_0^d e^{A_cT} B_c\, u[(k_{i-1})T]dt + \\ &\quad \int_0^{jT-d} e^{A_cT} B_c\, u(k_iT)dt \end{aligned}$$

or

$$x^d_{k_{i+1}} = A_j x_{k_i} + \Upsilon_0 B_c u(k_iT) + \Upsilon_1 B_c u[(k_{i-1})T]$$

To find the error $e^d(k_iT)$ between delayed and non-delayed system,

$$\begin{aligned} e^d(k_{i+1}T) &= \Upsilon_0 B_c u(k_iT) + \Upsilon_1 B_c u[(k_{i-1})T] - \\ &\quad B_j u(k_iT) \end{aligned}$$

Where,

$$\Upsilon_0(d) = \int_0^{jT-d} e^{A_ct}dt$$

$$\Upsilon(j,d) = e^{A_c(jT-d)} \int_0^d e^{A_ct}dt$$

$$\begin{aligned} e^d(k_{i+1}T) &= [\Upsilon_0(d)B_c - B_j]u(k_iT) + \\ &\quad \Upsilon_1(j,d)B_c u[(k_i-1)T] \\ e^d(k_{i+1}T) &= \begin{bmatrix} [\Upsilon_0(d)B_c - B_j] & \Upsilon_1(j,d)B_c \end{bmatrix} \\ &\quad \begin{bmatrix} u(k_iT) \\ u[(k_{i-1})T] \end{bmatrix} \end{aligned}$$

Similarly, when delay d is greater than jT and less than $2jT$, the error system can be written as,

$$\begin{aligned} e^d(k_{i+1}T) &= \begin{bmatrix} -B_j & \Upsilon_0(d)B_c & \Upsilon_1(j,d)B_c \end{bmatrix} \\ &\quad \begin{bmatrix} u(k_iT) \\ u[(k_{i-1})T \\ u[(k_{i-2})T] \end{bmatrix} \end{aligned}$$

Algorithm 1 Selection of N and Partitions of Delay Profile

$Min\_Norm = 99999$; ▷ Upper limit for Norm
$Max\_Iterations = 100$; ▷ Maximum number of iterations allowed
$Max\_Sections = 10$; ▷ Maximum number of partitions allowed i.e., N
for $N = 2$ **to** $Max\_Sections$ **do** ▷ Loop for choosing N
  for $i = 1$ **to** $Max\_Iterations$ **do**
    for $j = 1$ **to** $N - 1$ **do** ▷ Loop for choosing and optimizing boundaries
      Choose d_j *such that* $d_{j-1} < d_j < d_{j+1}$ *and* $P(j = 1) > 0.5$;
    end for
    for $a = 1$ **to** $N - 1$ **do**
      $W_a = P(j = a)$; ▷ Weights to allow comparison between Norms for different N
    end for
    $Norm = W_1 E[\Upsilon\Upsilon(1, d_1)] + W_2 E[\Upsilon\Upsilon(2, d_2)] + \ldots + W_{N-1} E[\Upsilon\Upsilon(N - 1, d_{N-1})]$;
    if $Norm <= Min\_Norm$ **then**
      $Min\_Norm = Norm$;
      $Boundary = [0, d_1, \ldots, d_{N-1}, T_d]$;
    end if
  end for
end for

Now, minimizing the mean error between delayed and non-delayed system reduces to the following condition:

$$min||E[\Upsilon\Upsilon(j, d)]||$$

where,

$$\begin{aligned} ||.|| &= \text{Matrix norm} \\ E[.] &= \text{Expected value} \\ \Upsilon\Upsilon(j, d) &= \begin{bmatrix} [\Upsilon_0(d)B_c - B_j] & \Upsilon_1(j, d)B_c \end{bmatrix} \end{aligned}$$

H_2 and H_∞ Norm are good measures that can be used to limit average and maximum gain provided by $\Upsilon\Upsilon$. Following steps can be used to obtain partitions of delay profile for good system performance:

- The most probable portion of delay profile that contains smaller delay values will be assigned sampling period T. This is necessary because this is the sampling period that is required to control the oscillatory modes as shown in this section. So, P(j=1)>0.5
- In case of large N, a disturbance occurring in between samples may deteriorate system performance because it will be detected on next measurement sample after period NT. This point should be considered while selecting N. If power system will be subjected to frequent variations, then N should be kept smaller.
- Use algorithm 1 with an appropriate linear optimization algorithm [23] to find the partitions of delay profile.
- Design observer based control. If it can't be designed try intuitive trimming of the boundaries or using a sub-optimal solution from algorithm 1 with greater value of $P(j = 1)$ or smaller value of N.

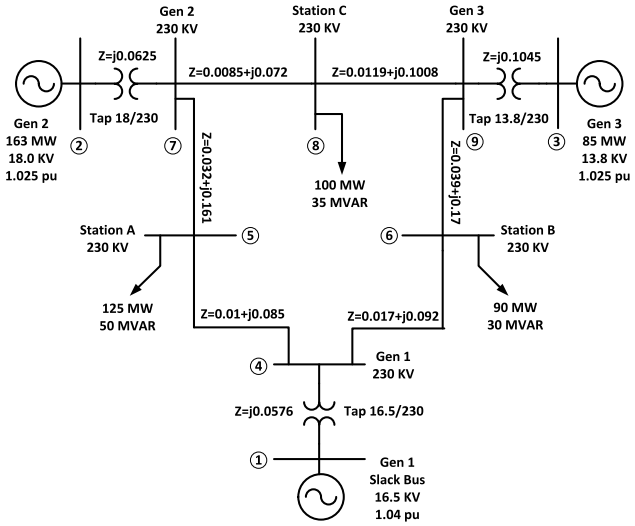

Figure 7: WSCC 3-machine, 9-bus system

6. Case Study

Consider the problem of small signal rotor-angle stability for the power system shown in Fig. 7 [16]. To represent dynamics of the generators, two-axis model is used with the IEEE type-I exciter. The details of the model and the parameters involved can be seen in [16]. The TCSC is installed between line 6 and 9 (from residue analysis). The parameters used for TCSC are $X_{cmax} = 0.07$, $X_{cmin} = -0.07$ and $T_c = 0.1s$.

Since small signal analysis is performed, the model of power system and TCSC is combined and then linearized. The dimension of state vector of the linearized system is reduced by referring the rotor angles of machine 2 and 3 (δ_2 and δ_3) to the rotor angle of machine 1 (δ_1). The eigenvalues analysis of the system shows that the system is stable but two pairs of eigenvalues are poorly damped causing oscillatory behavior. δ_{21} and

Table 1: Participation factors for δ_{21} and δ_{31} for dynamic modes of the power system

Eigenvalues	δ_{21}	δ_{31}
-1.0418± 12.9775j	0.1487	1
-0.2323± 7.4104j	1	0.3894
-5.3502± 9.9088j	0.0028	0.0099
-5.3094± 9.8694j	0.0003	0.005
-5.2383± 9.7879j	0.0006	0.0015
-6.3114	0.2468j	0.4894
-3.3038	0.0847j	0.3757
-3.7179	0.0770j	0.0504
-0.3556± 1.1737j	0.0013	0.0008
-0.5821	0.2799j	0.2168
-0.3506± 0.7297j	0.0028	0.0009
-0.3344± 0.5044j	0.0041	0.0182
-10	0	0

δ_{31} have high participation factors [16] in these modes as shown in Table 1. So, these modes need to be damped to control rotor angle deviations which may lead to instability. The outputs of the system are chosen here to be the rotor angles of machines 2 and 3, i.e., δ_{21} and δ_{31}. The linearized model is not reduced here since accuracy of the model is very important in the given design.Here, $n = 21$, $m = 2$, $k_u = 1$. The system is discretized at a faster sampling period $T = 0.2s$. It is calculated as mentioned in (28) using the power system mode having highest imaginary part of eigenvalues which in this case is $-1.0418 + 12.9775j$. The channel delay profile used is equally dividing maximum delay which is equal to sampling period T into five regions as shown in Fig. 8. Each region has uniform distribution with regional probabilities as 0.55, 0.2, 0.1, 0.1 and 0.05, respectively. Using the symmetry of delay profile the partitions to choose the sampling periods are kept same as the regional boundaries as shown in Fig. 8. The chosen sampling periods matches the criteria mentioned in section 5 and algorithm 1.

The discretized system is found to be controllable and observable. A switching observer based control is designed using Theorems 2 and 3. The response of the error system is shown in Fig. 9, where e_7, e_{14} and e_{21} are the errors corresponding to δ_{21}, δ_{31} and X_c; respectively. The error system is subjected to a random impulse disturbance and it can be seen that the states reach zero in less than $5s$. The closed-loop system with observer is subjected to non-zero random initial conditions to simulate load changes or momentarily fault on a tie line which trigger oscillations and the corresponding rotor angle deviations are shown in Fig. 10. Fig. 11 shows the reactance of TCSC. The rotor angles are given in radians and the reactance of TCSC is given

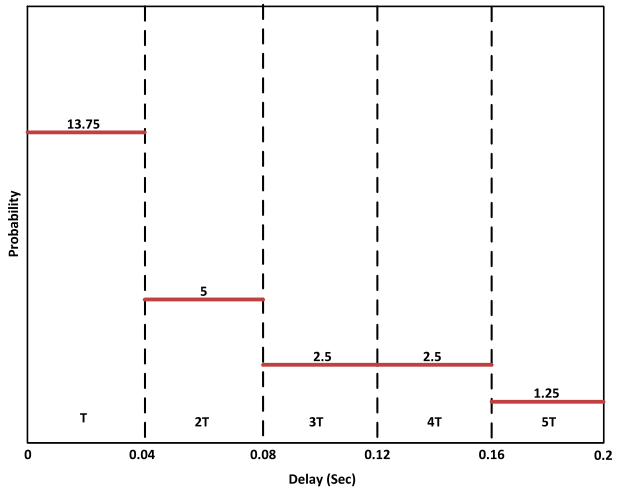

Figure 8: Delay profile used for case study along with partitions for selection of sampling periods

Table 2: Effect of change in $P(j = 5)$ on system settling time.

rr	Average Settling Time (sec)
0.1	6.8915
0.2	7.8505
0.3	8.3069
0.4	9.2193
0.5	9.2632

in p.u. The non-uniform measurement samples are shown along with continuous responses. It can be seen that performance of the closed-loop system is satisfactory. All oscillations damp out to zero in almost $4s$ with delays in the network. Whereas, the oscillations in uncontrolled system are clearly taking more than $10s$.

For detailed analysis of designed control, its robustness is verified through simulations. Average settling time (2% criterion) of δ_{21} over a number of simulations with same disturbance applied is used as a performance measure for robustness. Two factors are considered for this purpose. First is the probabilities of communication delays. They may change due to variations of physical condition of channel and the environment surrounding it. Second is the variation of model parameters. Change of eigenvalues can be observed due to modeling error and the conditions of components in power system, so, the performance of designed control is checked under the variation of model from the nominal model (which is used to design the controller).

Fig. 12 and Table 2 show the effect of change in delay probabilities on average settling time. Fig. 13 show the effect of change in power system model on average settling time. In Fig. 12, $P(j = 1)$ is decreased while increasing $P(j = 2)$. The result shows that the decrease in $P(j = 1)$ deteriorates the performance of controller but the controlled system still performs better than the uncontrolled system. Table 2 shows the average

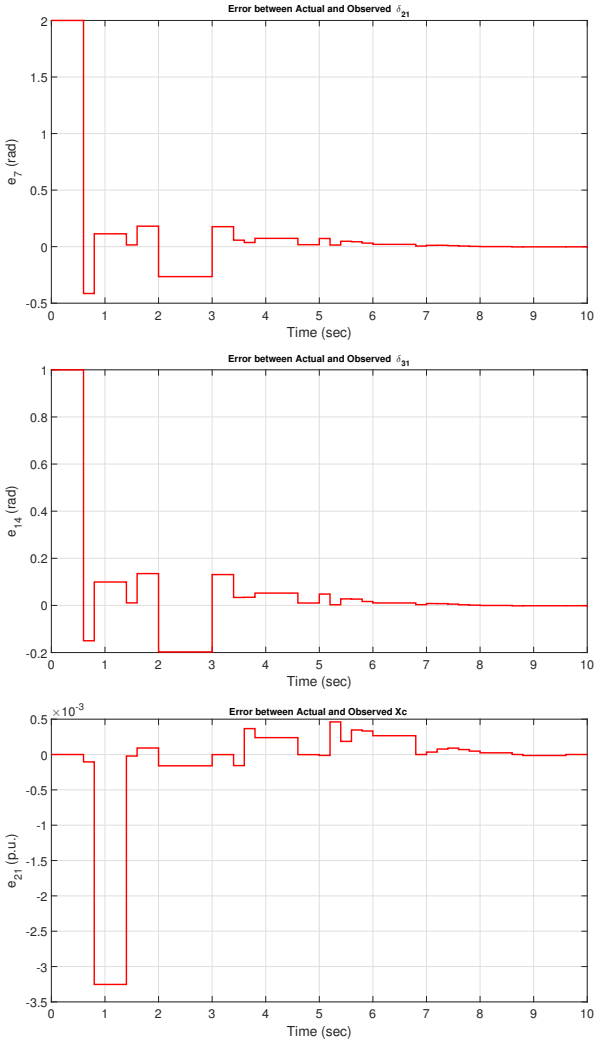

Figure 9: Error system subjected to non-zero initial conditions

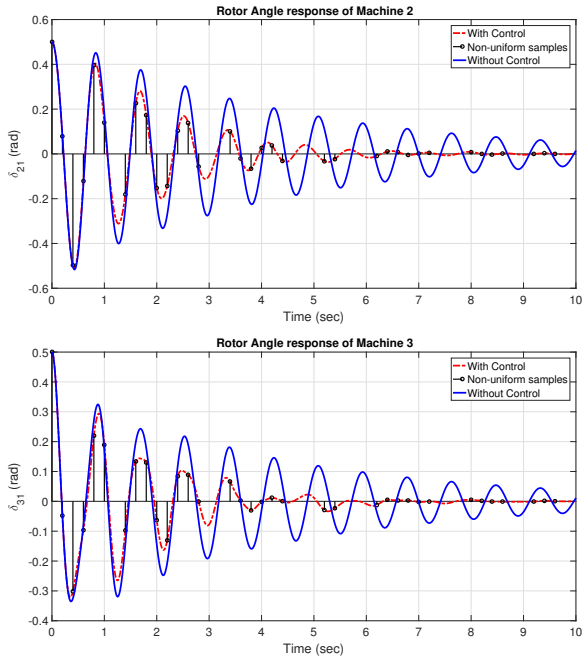

Figure 10: Rotor angle deviations when power system is subjected to random impulse disturbance.

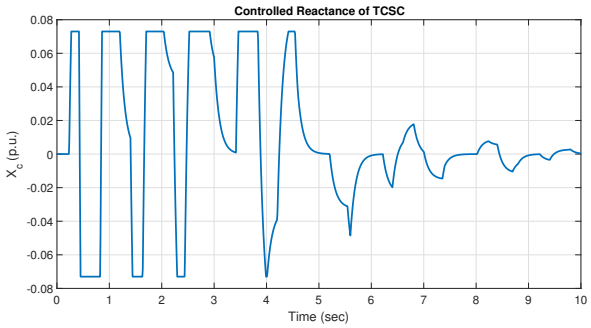

Figure 11: Reactance of TCSC when power system is subjected to random impulse disturbance.

settling time when $P(j = 5)$ is varied. A shifting variable rr is used for this purpose such that $P(j = 5) + rr$ and $P(j = jj) - rr$ are used as delay probabilities, where, $jj = 2, 3, 4, 5$. The average settling time of the closed loop system without control is $11.4429s$. It can be seen that it increases with the increase in rr, but it still does not cross the average settling time of uncontrolled system when $rr = 5$. It can be seen that even under big deviations delay profile, the response of controlled power system is superior than the uncontrolled system. In Fig.13, the system model is varied by shifting eigenvalues of continuous A_c matrix. Average settling time shows that the variation of A_c in both directions deteriorates the performance of controlled and uncontrolled system and it increases with more deviation of nominal eigenvalues. But, the performance of controlled system is far better than the uncontrolled system and the average settling time of controlled system also varies within the boundary of $2s$. Within the range of 10% change in eigenvalues, the closed-loop system damps the power system oscillations far better than the open-loop power system. When the eigenvalues deviate up to 16%, the uncontrolled system gets unstable but the controlled system stabilizes in $10s$ as shown in Fig. 14. Fig. 15 shows the corresponding reactance of TCSC. All the factors discussed above clearly demonstrate the effectiveness, robustness and superiority of the proposed control.

7. Conclusions

A non-uniformly sampled system is used here to reduce the effect of transmission delays in a bandwidth restricted channel on power system control. A switching observer based control is designed for the closed-loop system. The designed control give satisfactory performance in damping the oscillations. Moreover, under the changing conditions of power system and channel, the designed control gives better performance then the uncontrolled power system. It should be noted that the when the sampling time becomes large, observer is working without correction. Any disturbance occurring in between the this period will be detected on next measurement sample which may

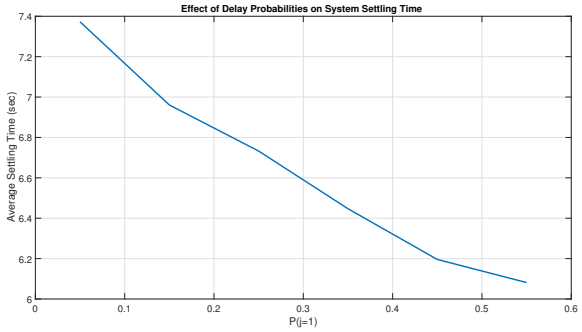

Figure 12: Effect of change in $P(j = 1)$ on the system settling time

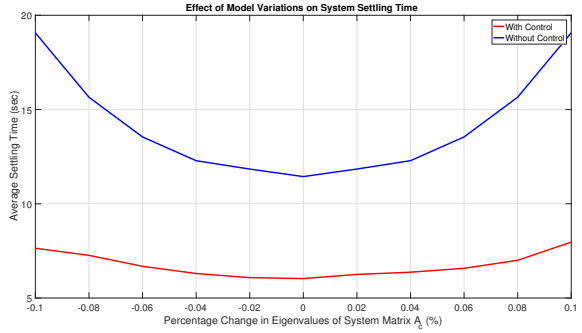

Figure 13: Effect of change in eigenvalues of system matrix A_c on the system settling time

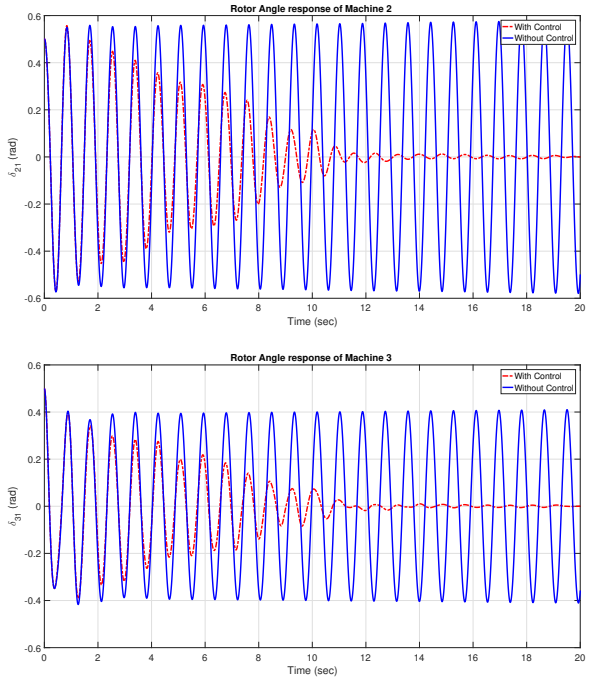

Figure 14: Rotor angle deviations when modified power system is subjected to random impulse disturbance.

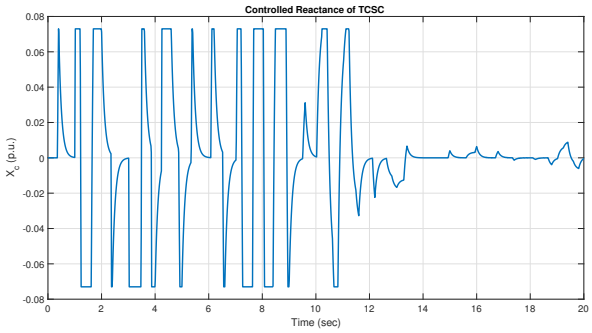

Figure 15: Reactance of TCSC when modified power system is subjected to random impulse disturbance.

effect the performance of closed loop system due to large duration. This imposes a limit on the maximum sampling period used NT.

Appendix A. Proof of Separation Principle

It is proved here that the system formed by plant and error dynamics have poles which can be independently placed by controller and observer [24]. Assume that the controller and observer gain matrices for different modes are same and can be represented as F and L respectively. The analysis performed will be simpler but it will also hold for the case of different gain matrices. So, using (6) in (5):

$$x_{k_{i+1}} = A^j x_{k_i} + BF\hat{x}_{k_{i+1}-1} + ABF\hat{x}_{k_{i+1}-2} + \ldots + A^{j-1}BF\hat{x}_{k_i}$$

Using (8), above equation can be written as

$$\begin{aligned} x_{k_{i+1}} &= A^j x_{k_i} + BF[(A+BF)^{j-1}\hat{x}_{k_i} + (A+BF)^{j-2} \\ &LC(x_{k_i} - \hat{x}_{k_i})] + ABF[(A+BF)^{j-2}\hat{x}_{k_i} + \\ &(A+BF)^{j-3}LC(x_{k_i} - \hat{x}_{k_i})] + \ldots + A^{j-2}BF \\ &[(A+BF)\hat{x}_{k_i} + LC(x_{k_i} - \hat{x}_{k_i})] + A^{j-1}BF\hat{x}_{k_i} \\ &= [A^j + BF(A+BF)^{j-1} + ABF(A+BF)^{j-2} \\ &+ \ldots + A^{j-2}BF(A+BF) + A^{j-1}BF]x_{k_i} + \\ &[-BF(A+BF)^{j-1} + BF(A+BF)^{j-2}LC - \\ &ABF(A+BF)^{j-2} + ABF(A+BF)^{j-3}LC \\ &- \ldots - A^{j-2}BF(A+BF) + A^{j-2}BFLC - \\ &A^{j-1}BF]e_{k_i} \end{aligned}$$

or

$$x_{k_{i+1}} = Z_{11}(j,F)x_{k_i} + Z_{12}(j,F,L)e_{k_i}$$

using (22) and above equation, the augmented system can be written in following form

$$\begin{bmatrix} x_{k_{i+1}} \\ e_{k_{i+1}} \end{bmatrix} = \begin{bmatrix} Z_{11}(j,F) & Z_{12}(j,F,L) \\ 0 & Z_{22}(j,L) \end{bmatrix} \begin{bmatrix} x_{k_i} \\ e_{k_i} \end{bmatrix}$$

Where, $Z_{22}(j, L) = A^j - A^{j-1}LC$. The characteristic equation of the system is

$$[sI - Z_{11}(j, F)]\,[sI - X_1(j, L)] = 0$$

Clearly, the eigenvalues can be independently placed by F and L, proving the Separation Principle.

References

[1] B. Pal, B. Chaudhuri, Robust control in power systems, Springer Science & Business Media, 2006.

[2] X. R. Chen, N. C. Pahalawaththa, U. D. Annakkage, C. S. Kumble, Controlled series compensation for improving the stability of multimachine power systems, IEE Proceedings - Generation, Transmission and Distribution 142 (4) (1995) 361–366, ISSN 1350-2360, doi:10.1049/ip-gtd:19951818.

[3] K. M. Son, J. K. Park, On the robust LQG control of TCSC for damping power system oscillations, IEEE Trans. Power Systems 15 (4) (2000) 1306–1312, ISSN 0885-8950, doi:10.1109/59.898106.

[4] J. Gao, Y. Xiao, J. Liu, W. Liang, C. P. Chen, A survey of communication/networking in smart grids, Future Generation Computer Systems 28 (2) (2012) 391–404.

[5] Y. Tipsuwan, M.-Y. Chow, Control methodologies in networked control systems, Control Engineering Practice 11 (10) (2003) 1099–1111.

[6] A. K. Singh, R. Singh, B. C. Pal, Stability Analysis of Networked Control in Smart Grids, IEEE Trans. Smart Grid 6 (1) (2015) 381–390, ISSN 1949-3053, doi:10.1109/TSG.2014.2314494.

[7] S. Wang, X. Meng, T. Chen, Wide-Area Control of Power Systems Through Delayed Network Communication, IEEE Trans. Control Systems Technology 20 (2) (2012) 495–503, ISSN 1063-6536, doi:10.1109/TCST.2011.2116022.

[8] H. Li, M. Y. Chow, Z. Sun, EDA-Based Speed Control of a Networked DC Motor System With Time Delays and Packet Losses, IEEE Trans. Industrial Electronics 56 (5) (2009) 1727–1735, ISSN 0278-0046, doi:10.1109/TIE.2009.2013749.

[9] N. R. Chaudhuri, D. Chakraborty, B. Chaudhuri, An Architecture for FACTS Controllers to Deal With Bandwidth-Constrained Communication, IEEE Trans. Power Delivery 26 (1) (2011) 188–196, ISSN 0885-8977, doi:10.1109/TPWRD.2010.2070881.

[10] G. Andersson, Modelling and analysis of electric power systems, ETH Zurich, september .

[11] P. Kansal, A. Bose, Bandwidth and Latency Requirements for Smart Transmission Grid Applications, IEEE Trans. Smart Grid 3 (3) (2012) 1344–1352, ISSN 1949-3053, doi:10.1109/TSG.2012.2197229.

[12] A. G. Phadke, J. S. Thorp, Communication needs for Wide Area Measurement applications, in: 5th International Conference on Critical Infrastructure (CRIS), 1–7, doi:10.1109/CRIS.2010.5617484, 2010.

[13] R. Javed, G. Mustafa, Power system stability enhancement over a network with random delays, in: 2015 Symposium on Recent Advances in Electrical Engineering (RAEE), 1–6, doi:10.1109/RAEE.2015.7352758, 2015.

[14] P. Kundur, N. J. Balu, M. G. Lauby, Power system stability and control, vol. 7, McGraw-hill New York, 1994.

[15] V. Sreeram, A. Ghafoor, Frequency weighted model reduction technique with error bounds, in: Proc. American Control Conference, ISSN 0743-1619, 2584–2589 vol. 4, doi:10.1109/ACC.2005.1470356, 2005.

[16] P. W. Sauer, Power system dynamics and stability, Prentice Hall, 1998.

[17] L. Xie, H. Yang, F. Ding, Inferential adaptive control for non-uniformly sampled-data systems, in: Proc. American Control Conference, ISSN 0743-1619, 4177–4182, doi:10.1109/ACC.2011.5991280, 2011.

[18] K. J. Åström, B. Wittenmark, Computer-controlled systems: theory and design, Courier Corporation, 2013.

[19] J.-Y. Yen, Y.-L. Chen, M. Tomizuka, Variable sampling rate controller design for brushless DC motor, in: Proc. 41st IEEE Conf. Decision and Control, vol. 1, ISSN 0191-2216, 462–467 vol.1, doi:10.1109/CDC.2002.1184539, 2002.

[20] G. Mustafa, T. Chen, $\mathcal{H}_\infty$ filtering for nonuniformly sampled systems: A Markovian jump systems approach, Systems & Control Letters 60 (10) (2011) 871–876.

[21] J. Daafouz, P. Riedinger, C. Iung, Stability analysis and control synthesis for switched systems: a switched Lyapunov function approach, IEEE Trans. Automatic Control 47 (11) (2002) 1883–1887, ISSN 0018-9286, doi:10.1109/TAC.2002.804474.

[22] L. E. Ghaoui, F. Oustry, M. AitRami, A cone complementarity linearization algorithm for static output-feedback and related problems, IEEE Trans. Automatic Control 42 (8) (1997) 1171–1176, ISSN 0018-9286, doi:10.1109/9.618250.

[23] X.-S. Yang, Flower pollination algorithm for global optimization, in: International Conference on Unconventional Computing and Natural Computation, Springer, 240–249, 2012.

[24] K. Ogata, Modern Control Engineering, Prentice-Hall, 2010.